



Bloch ferromagnetism of composite fermions

Md Shafayat Hossain ^{1,3} [∞], Tongzhou Zhao ^{1,2}, Songyang Pu², M. A. Mueed¹, M. K. Ma¹, K. A. Villegas Rosales¹, Y. J. Chung¹, L. N. Pfeiffer¹, K. W. West¹, K. W. Baldwin¹, J. K. Jain ¹ and M. Shayegan ¹ ¹ [∞]

In 1929, Felix Bloch suggested that the paramagnetic Fermi sea of electrons should make a spontaneous transition to a fully magnetized state at very low densities, because the exchange energy gained by aligning the spins exceeds the enhancement in the kinetic energy. However, experimental realizations of this effect have been hard to implement. Here, we report the observation of an abrupt, interaction-driven transition to full magnetization, highly reminiscent of Bloch ferromagnetism. Our platform utilizes the two-dimensional Fermi sea of composite fermions near half-filling of the lowest Landau level. We measure the Fermi wavevector—which directly provides the spin polarization—and observe a sudden transition from a partially spin-polarized to a fully spin-polarized ground state as we lower the density of the composite fermions. Our theoretical calculations that take Landau level mixing into account provide a semi-quantitative account of this phenomenon.

The ground state of a dilute system of electrons has long been a topic of theoretical fascination, because it represents a prototypical system with strong correlations¹⁻⁴. At low densities, the interaction energy dominates over the kinetic energy, thereby enhancing the importance of electron correlations. Wigner famously predicted an electron crystal at very low densities2, the search for which has driven many exciting developments. In another seminal paper¹, Bloch predicted that electrons should spontaneously magnetize at low densities, because the gain in exchange interaction energy due to the alignment of all spins outweighs the increase in kinetic energy. It is convenient to characterize the system with the dimensionless parameter r_s , the average inter-electron distance in units of the effective Bohr radius (equivalently, r_s is also the ratio of the Coulomb to Fermi energies). For a two-dimensional (2D) electron system, sophisticated quantum Monte Carlo calculations⁴ indicate that such a transition should occur when r_s exceeds 26, followed by another transition to a Wigner crystal state for $r_s > 35$. For 2D electrons, we have $r_s = (me^2/4\pi\hbar^2\varepsilon\varepsilon_0)/(\pi n)^{1/2}$, where m is the electron effective mass, ε is the dielectric constant and n is the electron density. Achieving a very dilute 2D electron system with low disorder, however, is extremely challenging. For example, in a GaAs 2D electron system ($m = 0.067m_0$ where m_0 is the free electron mass and $\varepsilon = 13$), $r_s \simeq 26$ corresponds to a density of $n \simeq 4.6 \times 10^8 \, \mathrm{cm}^{-2}$, which is indeed very difficult to attain^{5,6}. In GaAs 2D hole systems $(m \simeq 0.4 m_0)$, large r_s values can be reached more easily; in fact, hints of Wigner crystal formation near $r_s \simeq 35$ have been reported⁷. However, partly because of the strong spin-orbit interaction, extraction of the spin susceptibility and polarization of 2D holes is not straightforward8.

Although the spin polarization of interacting 2D electrons has always been of great interest, it was thrust into the limelight in the

1990s in the context of the enigmatic metal-insulator transition in dilute 2D carrier systems⁶⁻¹³. Numerous experiments revealed that spin and valley polarization in 2D carrier systems plays an important role in the temperature dependence of conductivity. There were even reports that the metal-insulator transition is linked to the full spin-polarization transition (for reviews see, for example, refs. 9,10). However, in a nearly ideal (single-valley, isotropic, very thin) 2D electron system confined to a narrow AlAs quantum well, it was observed that the spin susceptibility closely follows the results from the Monte Carlo calculations up to the highest experimentally achieved r_s (of ~10) and, importantly, remains finite as the 2D electron system goes through the metal-insulator transition at $r_s \simeq 8$ (ref. 11). It is fair to say that an experimental observation of the transition to full spin polarization, as manifested, for example, by a divergence of the spin susceptibility or a sudden increase in the Fermi wavevector, has been elusive so far¹²⁻¹⁴.

We report here the observation of a sudden, Bloch-type, interaction-driven transition to a fully magnetized ground state in a 2D system of composite fermions (CFs) near Landau level filling factor $\nu = 1/2$ as their density is reduced. These exotic, fermionic quasiparticles form in 2D electron systems exposed to a perpendicular magnetic field (B), and each is composed of two magnetic flux quanta and an electron 15-17. Although of a collective origin, CFs behave like ordinary fermions in many respects. At $\nu = 1/2$, having absorbed two flux quanta, the CFs act as if there is no external magnetic field and occupy a metallic Fermi sea state with a well-defined Fermi wavevector^{16,17}. Their Fermi sea and cyclotron orbits at small effective magnetic fields ($B^* = B - B_{\nu=1/2}$), and quantized energy levels at larger B^* , have been observed experimentally¹⁷. In our study, we probe the CF Fermi sea via geometric resonance measurements. The key idea is that when a weak, 1D periodic perturbation is applied to the 2D electron system, if the CFs can complete a cyclotron orbit without scattering, then they exhibit a geometric resonance when their orbit diameter equals the period of the perturbation (Fig. 1a). Such a resonance provides a direct and quantitative measure of the wavevector of the CFs16-22.

Our samples are 2D electron systems confined to modulation-doped, GaAs/AlGaAs heterostructures (grown by molecular beam epitaxy). The 2D electron density ranges from 10.16 to 2.20 in units of $10^{10}\,\rm cm^{-2}$, which we use throughout this Letter. In this density range $r_{\rm s}$ is 1.7–3.7 (see Methods for more details). We use a back gate to tune the density. In our geometric resonance measurements, we impose a small periodic density modulation, the estimated magnitude of which is less than ~0.5% (see Methods). As illustrated in Fig. 1a, this is achieved by fabricating a 1D, strain-inducing superlattice with period $a \simeq 200\,\rm nm$ on the surface of a lithographically defined Hall bar 22 .

NATURE PHYSICS LETTERS

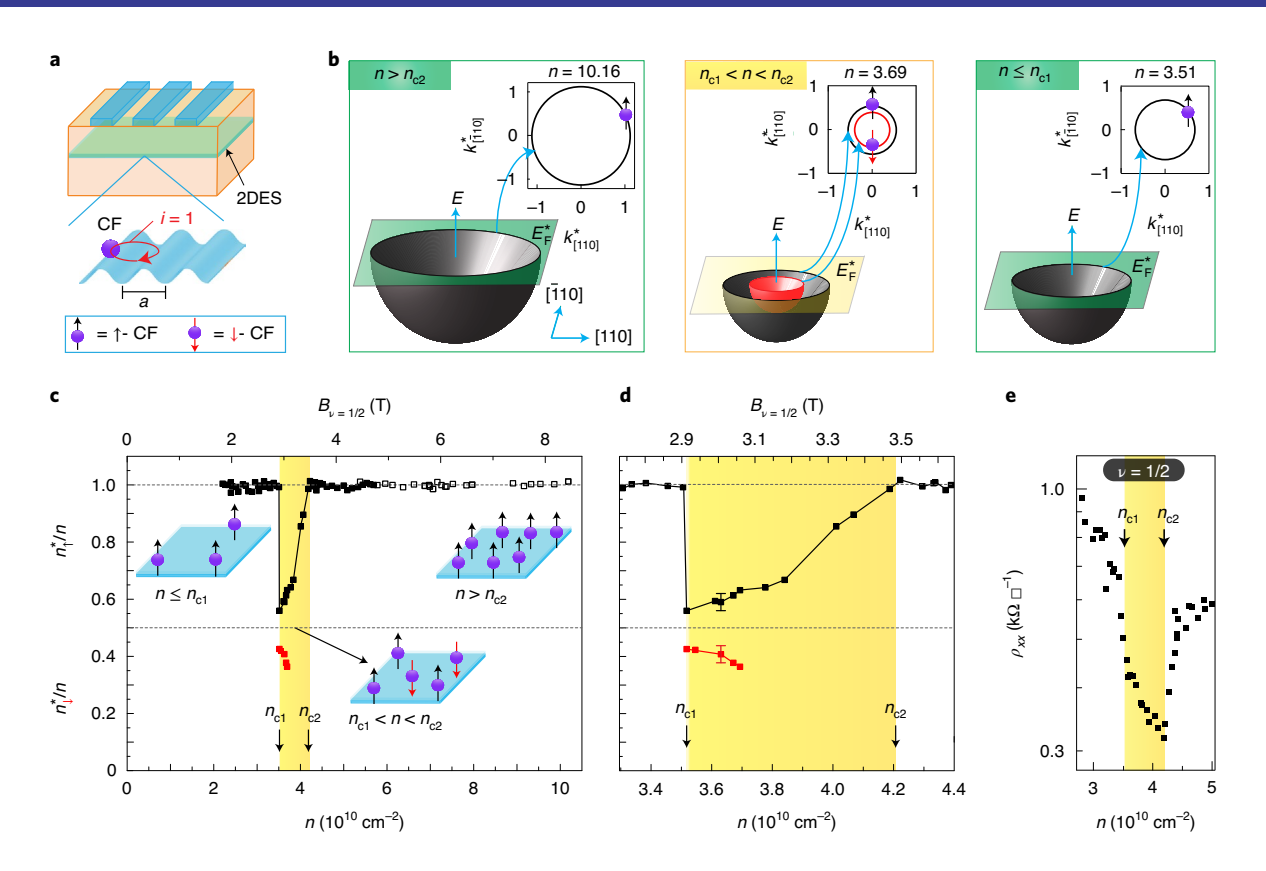


Fig. 1 [Evolution of the spin polarization of CFs as a function of electron density. **a**, Our experimental technique to probe the density of CFs, with a lateral surface superlattice of period *a* inducing a periodic density perturbation in the 2D electron system (2DES). When the cyclotron orbit of the CFs becomes commensurate with the period of the perturbation, the *i* = 1 geometric resonance occurs. **b**, Schematics of CF energy versus the wavevector. Cuts at the CF Fermi level (E_F^*) lead to circular Fermi contours, as shown in the insets (the units for $k_{(110)}$ and $k_{(110)}$ are 10^8 m⁻¹). These panels capture the evolution of the CF Fermi sea from fully magnetized to partially magnetized, then back to fully magnetized as we lower the density. Black and red contours denote the ↑-spin and ↓-spin CFs, respectively. The areas encircled by these Fermi contours yield the densities n_1^* and n_1^* of CFs with majority and minority spins, respectively. **c**, Measured n_1^* and n_1^* , normalized to *n*, plotted against *n*. At large *n*, the CFs are fully spin-polarized, that is, $n_1^*/n \simeq 1$. As the density is lowered below $n_{c2} \simeq 4.2$, the full spin polarization is lost and $n_1^*/n < 1$. However, at even lower densities, $n \le n_{c1} = 3.51$, the CFs experience an itinerant transition to a fully spin-polarized state. Filled and open squares represent data from two samples from different wafers. **d**, A magnified view of the yellow band ($n_{c1} < n < n_{c2}$) where the CFs are partially spin-polarized. Typical error bars (±4%) are also shown. **e**, Resistivity (ρ_{xx}) at $\nu = 1/2$ versus *n* for CFs. The pronounced minimum in ρ_{xx} in the yellow band signals that the CFs are partially spin-polarized in this density range (see Supplementary Section II.1 for details).

Figure 1b-e highlights our key experimental finding, showing the evolution of the CF Fermi sea and measured densities of CFs with majority (n_1^*) and minority (n_1^*) spin, normalized by the total electron density n, as n is varied. (Throughout this Letter, CF parameters are denoted by an asterisk.) At high densities $(n > n_c = 4.2)$, we find that CFs are fully spin-polarized, that is, $n_{\uparrow}^* = n$. This is consistent with previous reports¹⁷⁻²⁷. As is well documented experimentally and theoretically 17,26,27, at high densities, or equivalently high B, when the ratio (α) of the Zeeman energy ($E_Z = g\mu_B B$) to Coulomb energy $(E_C = e^2/4\pi\varepsilon\varepsilon_0 l_B)$, where $l_B = (\hbar/eB)^{1/2}$ exceeds a critical value $(\alpha_c \simeq 0.01)$, the CFs are fully spin-polarized. In our samples, $n_{c2} = 4.2$ corresponds to $\alpha \simeq 0.01$, in very good agreement with what is expected. As we lower n below 4.2, CFs lose their full spin polarization; this is also in accordance with previous measurements. Now, as the density is lowered even further, if the CFs are assumed to be non-interacting, one would expect the spin polarization to continue to decrease. There is no reason for the CFs to become fully spin-polarized again, because $\alpha = E_z/E_C$ is further decreased. However, as the density is lowered to $n_{c1} = 3.51$, CFs make a sudden transition back to a fully magnetized state. At even lower densities, the CFs remain fully magnetized. We attribute this transition to a Bloch-type, interaction-driven transition to a ferromagnetic state.

Next we describe how we deduce the degree of spin polarization for the CFs from geometric resonance measurements. When the CFs experience a small B^* , they orbit in a circular cyclotron motion with a radius of $R_{\rm c}^* = \hbar k_{\rm F}^*/eB^*$, the size of which is determined by the magnitude of the CFs' Fermi wavevector, $k_{\rm F}^*$. If the CFs have a sufficiently long mean-free path so they can complete a cyclotron orbit ballistically, then a geometric resonance occurs when the orbit diameter becomes commensurate with the period (a) of the perturbation (Fig. 1a). Quantitatively^{20–22}, when $2R_{\rm c}^*/a = i + 1/4$ (i = 1, 2, 3, ...), geometric resonances manifiest as minima in magneto-resistance at $B_i^* = 2\hbar k_{\rm F}^*/ea(i+1/4)$. Thus, $k_{\rm F}^*$ can be deduced directly from the positions of B_i^* . Using the measured $k_{\rm F}^*$, we can extract $n_{\rm T}^*$ and $n_{\rm T}^*$ from the relation $k_{\rm F}^* = (4\pi n_{\rm T, T}^*)^{1/2}$.

In Fig. 2, we focus on the densities close to $n_{\rm c1}$ and $n_{\rm c2}$ (Fig. 1c,d) and show representative magneto-resistance traces, each exhibiting well-developed geometric resonance features flanking a deep, V-shaped minimum at $\nu=1/2$. The traces in Fig. 2a, which show magneto-resistance over a large range of ν , attest to the high sample quality as evinced by the presence of fractional quantum Hall states, such as $\nu=1/3$ and 2/3, even at very low densities. In Fig. 2b we zoom in very close to $\nu=1/2$, and show the traces as a function of the effective magnetic field seen by the CFs, $B^*=B-B_{\nu-1/2}$.

LETTERS NATURE PHYSICS

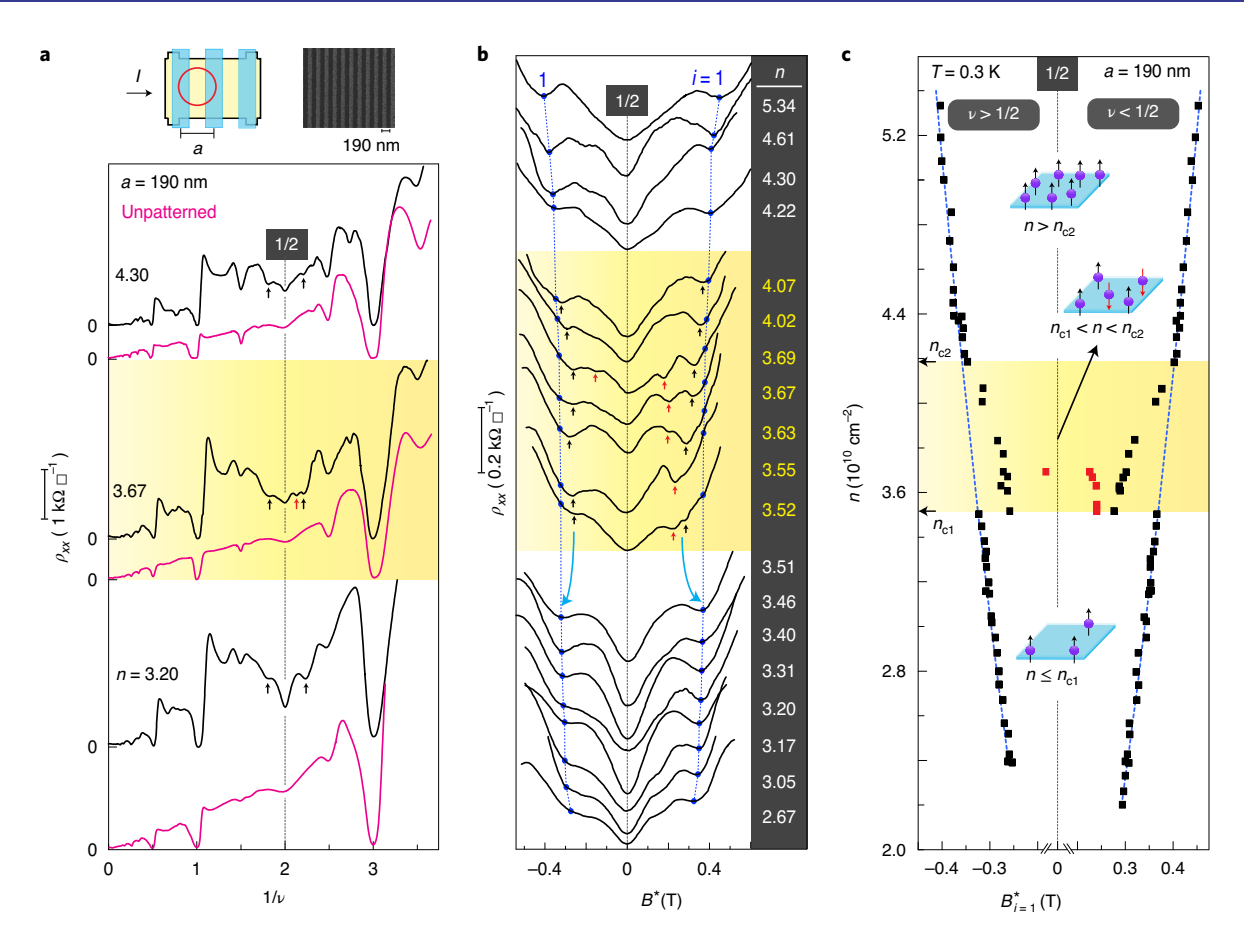


Fig. 2 | **Geometric resonance features of CFs near** ν =1/2. Magneto-transport traces, all taken at T = 0.30 K, are shown. In each panel, the traces are offset vertically for clarity and the electron densities, n, in units of 10^{10} cm⁻², are given for each trace. **a**, Data plotted against $1/\nu$ for three densities, one in each of the three regions ($n > n_{c2}$, $n_{c1} < n < n_{c2}$ and $n < n_{c2}$), showing well-developed fractional quantum Hall states. Traces taken from the section patterned with an a = 190 superlattice exhibit CF geometric resonance features near ν = 1/2, as demonstrated by the resistance minima flanking ν = 1/2 (marked by arrows). The unpatterned section (magenta) traces show no such features. The upper panel shows a schematic of the Hall bar and a representative scanning electron micrograph of the superlattice used in our measurements. **b**, Evolution of CF geometric resonance features near ν =1/2 with density. Blue dots mark the expected positions for the i = 1 geometric resonance for fully spin-polarized CFs. The yellow band in each panel indicates the $n_{c1} < n < n_{c2}$ region, where the CFs are only partially spin-polarized, and the locations of the CF geometric resonance minima (marked by vertical arrows) deviate from the blue dots. **c**, $B_{i=1}^*$ of CF geometric resonance plotted against n. The dotted blue curves show the expected $B_{i=1}^*$ as a function of n for fully spin-polarized CFs. Black and red squares denote the CF geometric resonance features corresponding to the two ↑ and ↓ spin species, respectively.

The geometric resonance minima are clearly seen in these traces at $|B^*| \simeq 0.2$ –0.5 T. In each trace, we mark the expected field positions of the i=1 CF geometric resonance (blue dots) assuming a fully spin-polarized CF Fermi sea. Note that, when CFs are fully spin-polarized, their density was found experimentally to be the minority carrier density (electrons for $\nu < 1/2$ and holes for $\nu > 1/2$). The expected positions marked by the blue dots in Fig. 2b traces are based on this assumption.

Starting from the highest density (uppermost trace, Fig. 2b), we note that the observed minima match the expected positions very well. This trend is seen in all the traces in the range $n > n_{c2}$. At lower densities, when $n_{c1} < n < n_{c2}$ (yellow band, Fig. 2b), however, the observed positions of the geometric resonance minima deviate from the $B_{i=1}^*$ expected for fully spin-polarized CFs and move closer to $\nu = 1/2$. Notably, at n = 3.69 and slightly lower densities, we observe two i = 1 geometric resonance minima on the $B^* > 0$ side of $\nu = 1/2$ (Fig. 2b). We associate these two minima with the i = 1 geometric resonance of CFs with different spins, and plot the deduced n_{\uparrow}^* and n_{\downarrow}^* in the yellow bands of Fig. 1c,d. Note that the sum of n_{\uparrow}^* and n_{\downarrow}^* equals the total density, as expected. (Note also that the double minima are observed primarily on the $B^* > 0$ side of

 $\nu=1/2$; we do not know the reason for this asymmetry.) As detailed in Supplementary Section II, we have additional evidence for the partial spin polarization of CFs in the range $n_{\rm cl} < n < n_{\rm c2}$. The evidence includes geometric resonance data taken in tilted magnetic fields (Fig. 3 and Supplementary Fig. 3) and also the observation of a pronounced minimum in the resistivity of the CFs at $\nu=1/2$ in the density range $n_{\rm cl} < n < n_{\rm c2}$ (Fig. 1e and Supplementary Fig. 2). The minimum is consistent with the enhanced screening of the disorder potential when the CFs are partially spin-polarized (see Supplementary Section II.1 for details).

The most important finding of our data is captured below the yellow band in Fig. 2b. When the density is lowered below 3.52, the traces near $\nu=1/2$ suddenly become simple again and, most notably, the positions of the observed geometric resonance minima on the two sides of $\nu=1/2$ agree very well with the expected $B_{i=1}^*$ for fully spin-polarized CFs (blue dots). This observation provides direct and quantitative evidence that CFs at very low densities make a sudden transition to a fully magnetized state. We summarize the measured $B_{i=1}^*$ as a function of n in Fig. 2c. Figure 2c illustrates that starting from the highest density and down to n_{c2} , $B_{i=1}^*$ follows the blue curves, which denote the expected $B_{i=1}^*$ for full spin

NATURE PHYSICS LETTERS

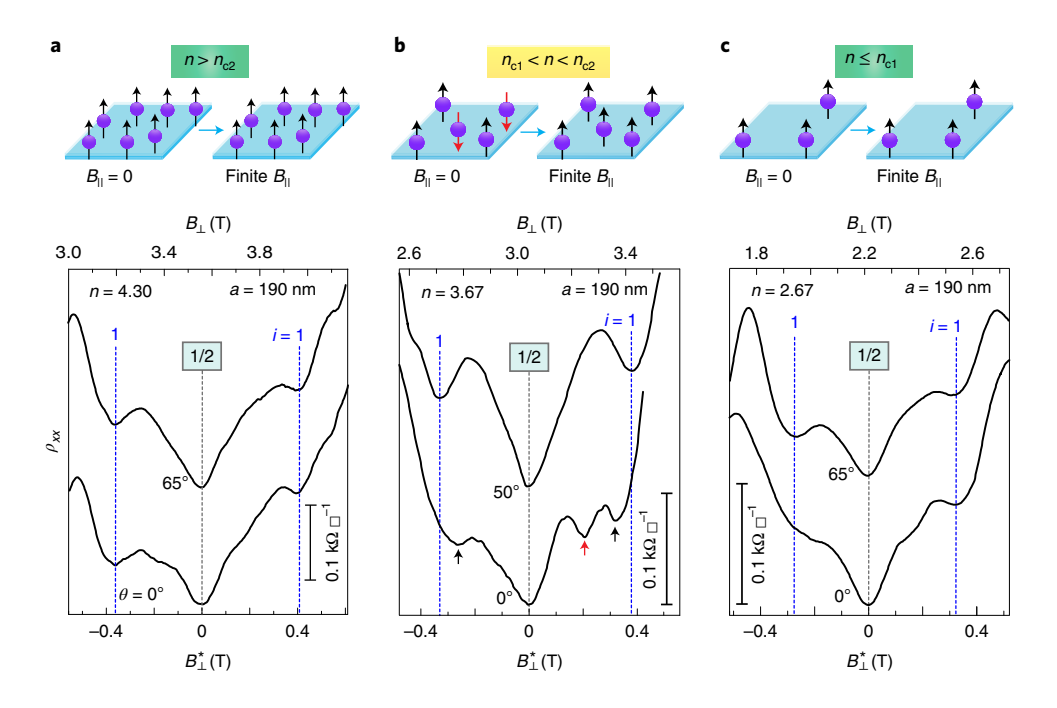


Fig. 3 | **Tilt evolution of the CF geometric resonance features near** ν = 1/2. **a**-**c**, Data are shown for n = 4.30 (**a**), n = 3.67 (**b**) and n = 2.67 (**c**). Traces are offset vertically for clarity and the tilt angle θ is given for each trace. The expected positions for the i = 1 geometric resonances for fully magnetized CFs are marked with vertical blue lines. In all three panels, the scale for the applied external field B_{\perp} is shown on the top axis, while the bottom scale is the effective magnetic field B_{\perp}^* experienced by the CFs. At n = 3.67 (**b**), CFs near ν = 1/2 are partially spin-polarized, as evinced from the CF geometric resonance minima marked by arrows. However, in the presence of a sufficiently large B_{\parallel} (see the θ = 50° trace), the two minima on the B^* > 0 side disappear and are replaced by a single minimum whose position aligns with the expected position for fully spin-polarized CFs. The position of the geometric resonance minimum on the B^* < 0 side also moves to the expected fully polarized position. These traits are consistent with the presence of a partially polarized state for n_{c1} < n < n < n < n < n < n < n < n < n < n < n < n < n < n < n < n < n < n < n < n < n < n < n < n < n < n < n < n < n < n < n < n < n < n < n < n < n < n < n < n < n < n < n < n < n < n < n < n < n < n < n < n < n < n < n < n < n < n < n < n < n < n < n < n < n < n < n < n < n < n < n < n < n < n < n < n < n < n < n < n < n < n < n < n < n < n < n < n < n < n < n < n < n < n < n < n < n < n < n < n < n < n < n < n < n < n < n < n < n < n < n < n < n < n < n < n < n < n < n < n < n < n < n < n < n < n < n < n < n < n < n < n < n < n < n < n < n < n < n < n < n < n < n < n < n < n < n

polarization. For $n_{c1} < n < n_{c2}$, $B_{i=1}^*$ deviates gradually from the blue curves (see the yellow band), indicating a loss of magnetization. Finally, below n_{c1} , $B_{i=1}^*$ suddenly aligns with the blue curves, signalling a Bloch-like transition to full spin polarization.

The experimental results described in Figs. 1–3 prompted us to perform a detailed theoretical investigation of the spin physics of the CF liquid at $\nu=1/2$ as a function of density. If one neglects the effect of Landau level mixing and considers an ideal 2D electron system with zero layer thickness, then both the inter-CF interaction and the CF kinetic energies are proportional to the Coulomb energy, which is the only scale in the problem. In this case, the transition from a fully spin-polarized state to a partially polarized state occurs at a density-independent value of E_Z/E_C and, as seen in the following, no Bloch transition occurs at $\nu=1/2$ as a function of density. The transition seen at $\nu=1/2$ is therefore probably driven by Landau level mixing, which alters the residual interaction between CFs in a complicated manner. The parameter r_s characterizes the strength of Landau level mixing; for $\nu=1/2$ we have $r_s=2\kappa$, where $\kappa=E_C/\hbar\omega_c$ is the standard Landau level mixing parameter.

We incorporate Landau level mixing through the non-perturbative, fixed-phase, diffusion Monte Carlo method²⁸ (see Supplementary Section V for details). This method has been employed previously to study the role of Landau level mixing on spin polarization of the fractional quantum Hall states²⁹ and the stability of the crystal state at low fillings^{28,30}. We assume zero layer thickness—this should be a good first-order approximation because the transverse wavefunction in the heterojunction geometry is narrow, and also because corrections due to Landau level mixing are more important than finite-width corrections for the parameters of interest. The

calculated changes (Supplementary Section V.3) in the energies per particle for the fully spin-polarized and spin-singlet CF Fermi seas, $\Delta E_{\rm p}(r_{\rm s}) = E_{\rm p}(r_{\rm s}) - E_{\rm p}(0)$ and $\Delta E_{\rm s}(r_{\rm s}) = E_{\rm s}(r_{\rm s}) - E_{\rm s}(0)$, respectively, are shown in the inset of Fig. 4. It is notable that $E_{\rm p}$ decreases faster than $E_{\rm s}$ with increasing $r_{\rm s}$, which is what causes the Bloch transition.

A direct comparison with experiment requires a consideration of E_7 . In the Stoner model of itinerant ferromagnetism³, which considers a contact interaction between oppositely spin-polarized CFs, the fully spin-polarized state is predicted to occur (Supplementary Section V.4) for $E_Z \ge E_Z^{\text{crit}} \equiv 4(E_p - E_s)$, where E_Z^{crit} is the critical Zeeman energy. From our diffusion Monte Carlo calculation (inset, Fig. 4) we estimate $E_p(r_s) - E_s(r_s) = E_p(0) - E_s(0) - \gamma r_s E_C$ with $\gamma = 0.0012(2)$, which gives $E_Z^{crit}(r_s) = E_Z^{crit}(0) - 4\gamma r_s E_C$. With $E_Z^{\text{crit}}(0) = 0.022E_C$ taken from an earlier calculation²⁷, the resulting $E_7^{\text{crit}}(r_s)$ lies in the shaded red region in Fig. 4. A phase transition occurs when E_z , shown by the solid blue line, crosses E_z^{crit} . Our calculation admits the possibility of two transitions in the vicinity of $r_s \approx 2.8$, which corresponds to $n \approx 4.2 \times 10^{10} \,\mathrm{cm}^{-2}$ for parameters of GaAs. Given the various approximations and assumptions made in our model and the microscopic diffusion Monte Carlo calculations, and given that E_Z^{crit} depends sensitively on very small energy differences (which are merely a fraction of 1% of the energies of the individual states), our theory should be considered only semi-quantitative, but it brings out the qualitative physics underlying the Bloch transition of CFs. The analysis presented in Supplementary Section V.4 shows that transitions at the experimentally observed densities n_{c1} and n_{c2} can be obtained by fitting the values of γ and $E_Z^{\text{crit}}(r_s = 0)$, which are in reasonable proximity to those obtained from the microscopic calculation.

LETTERS NATURE PHYSICS

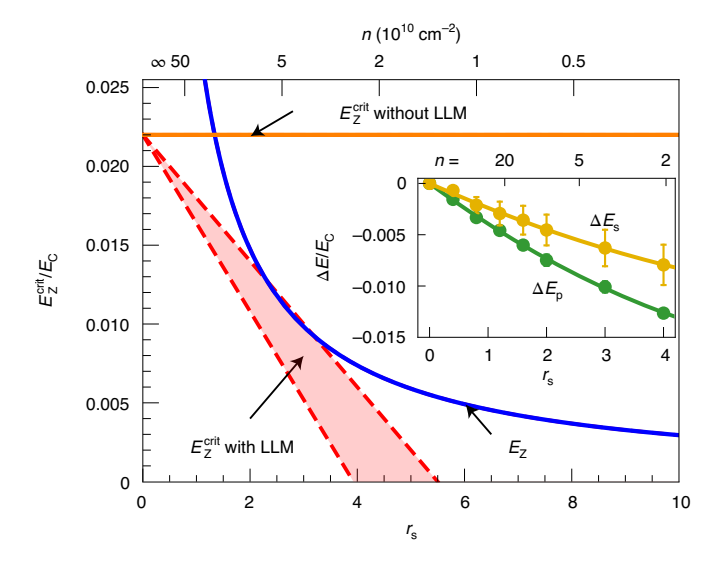


Fig. 4 | The critical Zeeman energy E_Z^{crit} as a function of r_s or nfor fixed filling factor $\nu = 1/2$. Note that n and r_s are related as $n \approx (32.8/r_c^2) \times 10^{10}$ cm⁻² for parameters appropriate for GaAs 2D electron systems. All plotted energies are normalized to the Coulomb energy (E_C) . The horizontal orange line shows E_Z^{crit} without Landau level mixing, whereas E_7^{crit} with Landau level mixing lies in the red region (indicating the statistical uncertainty in our diffusion Monte Carlo calculation). The system is predicted to be fully spin-polarized when the Zeeman energy E_7 (blue line) exceeds E_7^{crit} . These results admit the possibility of two phase transitions in the vicinity of $r_s \approx 2.8$ or $n \approx 4.2 \times 10^{10}$ cm⁻². The inset shows $\Delta E_p(r_s) = E_p(r_s) - E_p(r_s = 0)$ and $\Delta E_s = E_s(r_s) - E_s(r_s = 0)$, respectively, that is, changes in the energies (per particle) of the fully polarized and spin-singlet states as a function of Landau level mixing, obtained by extrapolating the energies of finite-size systems to the thermodynamic limit (Supplementary Section V.3). The calculated behaviour, $\Delta E_p(r_s) - \Delta E_s(r_s) \approx -\gamma r_s E_C$ with $\gamma = 0.0012(2)$, is used to determine E_7^{crit} , as explained in the main text. LLM refers to Landau level mixing.

For E_z = 0, which can, in principle, be achieved by application of hydrostatic pressure, theory predicts a fully spin-polarized state for $r_s > 4.6(6)$ (Fig. 4). One may ask why the Bloch transition for CFs should occur at a relatively small value of r_s (compared to $r_s \approx 26$ for electrons). The value of r_s where the Bloch transition occurs for CFs is determined by a complex interplay between the inter-CF interaction, a remnant of the Coulomb interaction between electrons, and the CF kinetic energy. Intuitively, one factor that reduces the critical r_s for CFs is their large mass (compared to the electron band mass), which diminishes the importance of the CF kinetic energy.

Online content

Any methods, additional references, Nature Research reporting summaries, source data, extended data, supplementary information, acknowledgements, peer review information; details of author contributions and competing interests; and statements of data and code availability are available at https://doi.org/10.1038/s41567-020-1000-z.

Received: 5 February 2020; Accepted: 8 July 2020; Published online: 17 August 2020

References

1. Bloch, F. Z. Bemerkung zur Elektronentheorie des Ferromagnetismus und der elektrischen Leitfähigkeit. Z. Phys. 57, 545–555 (1929).

- Wigner, E. On the interaction of electrons in metals. Phys. Rev. 46, 1002–1011 (1934).
- 3. Stoner, E. C. Ferromagnetism. Rep. Prog. Phys. 11, 43-112 (1947).
- Attaccalite, C., Moroni, S., Gori-Giorgi, P. & Bachelet, G. B. Correlation energy and spin polarization in the 2D electron gas. *Phys. Rev. Lett.* 88, 256601 (2002).
- Sajoto, T., Suen, Y. W., Engel, L. W., Santos, M. B. & Shayegan, M. Fractional quantum Hall effect in very-low-density GaAs/Al_xGa_{1-x}As heterostructures. *Phys. Rev. B* 41, 8449–8460 (1990).
- Zhu, J., Stormer, H. L., Pfeiffer, L. N., Baldwin, K. W. & West, K. W. Spin susceptibility of an ultra-low-density two-dimensional electron system. *Phys. Rev. Lett.* 90, 056805 (2003).
- Yoon, J., Li, C. C., Shahar, D., Tsui, D. C. & Shayegan, M. Wigner crystallization and metal-insulator transition of two-dimensional holes in GaAs at B=0. Phys. Rev. Lett. 82, 1744–1747 (1999).
- Winkler, R. et al. Anomalous spin polarization of GaAs two-dimensional hole systems. Phys. Rev. B 72, 195321 (2005).
- Kravchenko, S. V. & Sarachik, M. P. Metal-insulator transition in two-dimensional electron systems. Rep. Prog. Phys. 67, 1–44 (2004).
- Spivak, B., Kravchenko, S. V., Kivelson, S. A. & Gao, X. P. A. Colloquium: transport in strongly correlated two-dimensional electron fluids. *Rev. Mod. Phys.* 82, 1743–1766 (2010).
- Vakili, K., Shkolnikov, Y. P., Tutuc, E., De Poortere, E. P. & Shayegan, M. Spin susceptibility of two-dimensional electrons in narrow AlAs quantum wells. *Phys. Rev. Lett.* 92, 226401 (2004).
- Pudalov, V. M., Kutsevich, A. Y., Gershenson, M. E., Burmistrov, I. S. & Reznikov, M. Probing spin susceptibility of a correlated two-dimensional electron system by transport and magnetization measurements. *Phys. Rev. B* 98, 155109 (2018).
- Li, S., Zhang, Q., Ghaemi, P. & Sarachik, M. P. Evidence for mixed phases and percolation at the metal-insulator transition in two dimensions. *Phys. Rev. B* 99, 155302 (2019).
- Vermeyen, E., Sá de Melo, C. A. R. & Tempere, J. Exchange interactions and itinerant ferromagnetism in ultracold Fermi gases. *Phys. Rev. A* 98, 023635 (2018).
- Jain, J. K. Composite-fermion approach for the fractional quantum Hall effect. Phys. Rev. Lett. 63, 199–202 (1989).
- Halperin, B. I., Lee, P. A. & Read, N. Theory of the half-filled Landau level. *Phys. Rev. B* 47, 7312–7344 (1993).
- 17. Jain, J. K. Composite Fermions (Cambridge Univ. Press, 2007).
- Willett, R. L., Ruel, R. R., West, K. W. & Pfeiffer, L. N. Experimental demonstration of a Fermi surface at one-half filling of the lowest Landau level. *Phys. Rev. Lett.* 71, 3846–3849 (1993).
- Kang, W., Stormer, H. L., Pfeiffer, L. N., Baldwin, K. W. & West, K. W. How real are composite fermions? *Phys. Rev. Lett.* 71, 3850–3853 (1993).
- Willett, R. L., West, K. W. & Pfeiffer, L. N. Geometric resonance of composite fermion cyclotron orbits with a fictitious magnetic field modulation. *Phys. Rev. Lett.* 83, 2624–2627 (1999).
- Smet, J. H. et al. Commensurate composite fermions in weak periodic electrostatic potentials: direct evidence of a periodic effective magnetic field. *Phys. Rev. Lett.* 83, 2620–2623 (1999).
- Kamburov, D. et al. What determines the Fermi wave vector of composite fermions? *Phys. Rev. Lett.* 113, 196801 (2014).
- Dementyev, A. E. et al. Optically pumped NMR studies of electron spin polarization and dynamics: new constraints on the composite fermion description of ν = 1/2. Phys. Rev. Lett. 83, 5074–5077 (1999).
- 24. Melinte, S. et al. NMR determination of 2D electron spin polarization at ν = 1/2. *Phys. Rev. Lett.* **84**, 354–357 (2000).
- Tracy, L. Á., Eisenstein, J. P., Pfeiffer, L. N. & West, K. W. Spin transition in the half-filled Landau level. *Phys. Rev. Lett.* 98, 086801 (2007).
- Liu, Y. et al. Spin polarization of composite fermions and particle-hole symmetry breaking. Phys. Rev. B 90, 085301 (2014).
- Park, K. & Jain, J. K. Phase diagram of the spin polarization of composite fermions and a new effective mass. *Phys. Rev. Lett.* 80, 4237–4240 (1998).
- Ortiz, G., Ceperley, D. M. & Martin, R. M. New stochastic method for systems with broken time-reversal symmetry: 2D fermions in a magnetic field. *Phys. Rev. Lett.* 71, 2777–2780 (1993).
- Zhang, Y., Wójs, A. & Jain, J. K. Landau-level mixing and particle-hole symmetry breaking for spin transitions in the fractional quantum Hall effect. *Phys. Rev. Lett.* 117, 116803 (2016).
- Zhao, J., Zhang, Y. & Jain, J. K. Crystallization in the fractional quantum Hall regime induced by Landau-level mixing. Phys. Rev. Lett. 121, 116802 (2018).

Publisher's note Springer Nature remains neutral with regard to jurisdictional claims in published maps and institutional affiliations.

© The Author(s), under exclusive licence to Springer Nature Limited 2020

NATURE PHYSICS LETTERS

Methods

Our samples are 2D electron systems confined to modulation-doped GaAs/ AlGaAs heterostructures grown by molecular beam epitaxy. The 2D electron systems are buried 190 nm under the surface to ensure good sample quality. They have densities (n) ranging from 10.16 to 2.20 in units of 10^{10} cm⁻², which we use throughout. The low-temperature mobilities (μ) of our samples are in the range 1.1-0.5 in units of $10^7\,\text{cm}^2\,\text{V}^{-1}\,\text{s}^{-1}$, which are very high and therefore favourable to ballistic transport of CFs. This is a necessary condition for observing the geometric resonance features. For our measurements, Hall bar samples were fabricated using standard photolithography techniques, and alloyed InSn contacts were used to contact the 2D electron systems. The samples comprise multiple Hall bar sections, each of length 100 μm and width 50 μm. Via electron-beam lithography and using a calixarene-based negative electron-beam resist, we patterned the sample surface with strain-inducing superlattices perpendicular to the current direction. Thanks to the piezoelectric effect in GaAs, the periodic strain from this surface superlattice propagates to the 2D electron system and leads to a small density modulation. The availability of multiple sections enables us to study different superlattice periods in the same sample. The different sections are patterned with periods ranging from 190 to 225 nm. Finally, we fitted each sample with an In back gate to tune the electron density.

The measurements were carried out in a 3He cryostat with a base temperature of 0.3 K by passing current (I = 10 nA, 13 Hz) perpendicular to the density modulation. Note that we injected a very low measurement current to avoid polarizing the nuclear spins, which might introduce an effective nuclear field to our 2D electron system, thus affecting the electron Zeeman splitting25. We also checked the up and down magnetic field sweeps and did not observe any noticeable hysteresis. Such absence of hysteresis is indeed expected from a system of CFs. In that context, it is important to note that CFs, by necessity, require a finite magnetic field to emerge. When the CFs become fully spin-polarized, it makes most sense that the direction of their aligned spins is determined by the direction of the applied magnetic field. Therefore, as we sweep the magnetic field about $\nu = 1/2$ (or the position of the geometric resonance features), one would not expect magnetic domains or hysteresis. We also stress that the relevant magnetic field for the spin polarization of the CFs is the total applied magnetic field B (ref. ¹⁷), which is always non-zero, and not the effective field B^* (which passes through zero as one goes from $\nu > 1/2$ to $\nu < 1/2$).

Next we discuss the periodic potential modulation, which we impose on CFs for geometric resonance measurements. The strength of this modulation depends on the depth of the 2D electrons from the surface and the period of the superlattice. For periods shorter than the depth of the 2D electrons, the higher harmonics of the potential modulation are attenuated, resulting in a weaker modulation amplitude (see ref. ³¹ and references therein). Following the same analysis as in ref. ³¹, we can obtain a reasonable estimate of the strength of this periodic modulation. We normalized the superlattice period to the depth of the 2D electrons (190 nm for our samples) and then compared it to the 2D electrons at 135-nm depth used in ref. ³¹. The strength of our 190-nm-period modulation turns out to be less than 0.5%.

We stress that the period of the superlattice required to observe clear geometric resonance features depends on the electron density and the depth of the 2D electron system. This is because the CFs are fragile and require a very gentle modulation to exhibit clear geometric resonance features ³². In our samples, the depth of the 2D electron system is fixed and equals 190 nm. On the other hand, we tune the density by applying voltages to the back gate. Therefore, to observe clear geometric resonance features in all the densities in our experiments, we use superlattices of different periods depending on the electron density. For densities down to $n \simeq 7.05$, we observe clear geometric resonance features for a = 225 and 200 nm. For lower densities we use a = 200 nm (for $n \simeq 6.99$ to 5.34) and a = 190 nm (for n = 5.57 to 2.26) to ensure an appropriate modulation.

Extended Data Fig. 1 presents magneto-resistance traces for the sample patterned with a=190 nm for four different densities in the ranges $n>n_{c_2}$, $n_{c_1} < n < n_{c_2}$ and $n \le n_{c_1}$ and compare them with the corresponding unpatterned (reference) section of the Hall bar. Although small, the impact of the periodic modulation created by the a=190 nm superlattice manifests in the magneto-resistance traces as a V-shaped minimum at $\nu=1/2$, flanked by minima

on both sides of $\nu=1/2$, which signal the geometric resonance of CFs with the periodic potential (upper traces in Extended Data Fig. 1). On the other hand, as seen from the lower traces in all four panels of Extended Data Fig. 1, the unpatterned section exhibits no such features flanking $\nu=1/2$. We note that the V-shaped minimum at $\nu=1/2$ in the a=190 nm traces, that is, the positive magneto-resistance around half-filling, is attributed to open orbits of CFs, analogous to the open orbits of carriers in the classical magnetic breakdown mechanism^{21,22}.

Finally, as seen in Fig. 2b, the traces show pronounced geometric resonance minima on the $\nu < 1/2$ ($B^* > 0$) side down to very low densities ($n \simeq 2.7$). Therefore, we can extract the location of the geometric resonance minima on the $\nu < 1/2$ side with good accuracy. On the other hand, at densities below $n \simeq 2.7$, and especially on the $\nu > 1/2$ ($B^* < 0$) side, the CF geometric resonance minima are less pronounced. Therefore, to accurately extract the $B^*_{i=1}$ for $n \lesssim 2.7$, we perform a simple background subtraction process. We emphasize that this extraction process is done for densities $n \lesssim 2.7$ that are well below $n = n_{\rm cl}$ where the Bloch transition occurs. Therefore, it has no bearing on our conclusions.

Data availability

Data that support the plots within this paper and other findings of this study are available from the corresponding author upon reasonable request. Source data are provided with this paper.

References

- Mueed, M. A. et al. Reorientation of the stripe phase of 2D electrons by a minute density modulation. *Phys. Rev. Lett.* 117, 076803 (2016).
- Hossain, M. S. et al. Direct observation of composite fermions and their fully-spin-polarized Fermi sea near ν=5/2. Phys. Rev. Lett. 120, 256601 (2018).

Acknowledgements

We acknowledge support through the the National Science Foundation (grant DMR 1709076) for measurements and the US Department of Energy Basic Energy Science (grant DEFG02-00-ER45841), the National Science Foundation (grants ECCS 1906253 and MRSEC DMR 1420541) and the Gordon and Betty Moore Foundation's EPiQS Initiative (grant GBMF9615) for sample fabrication and characterization. The theoretical work at Penn State (T.Z., S.P. and J.K.J.) was supported in part by the US Department of Energy, Office of Basic Energy Sciences, under grant no. DE-SC0005042. J.K.J. thanks the Indian Institute Science, Bangalore, where part of this work was performed, for their hospitality, and the Infosys Foundation for making the visit possible. M.S. acknowledges a QuantEmX travel grant from the Institute for Complex Adaptive Matter (ICAM) and the Gordon and Betty Moore Foundation through grant no. GBMF5305. We also thank R. Warburton and R. Winkler for illuminating discussions.

Author contributions

M.S.H. fabricated the devices, performed the measurements and analysed the data. M.S.H., M.A.M., J.K.J. and M.S. discussed the data. T.Z., S.P. and J.K.J. performed the theoretical calculations. Y.J.C., L.N.P., K.W.W. and K.W.B. grew the quantum well samples via molecular beam epitaxy. M.K.M. and K.A.V.R. helped with the measurements. M.S.H., T.Z., S.P., J.K.J. and M.S. co-wrote the manuscript with input from all co-authors.

Competing interests

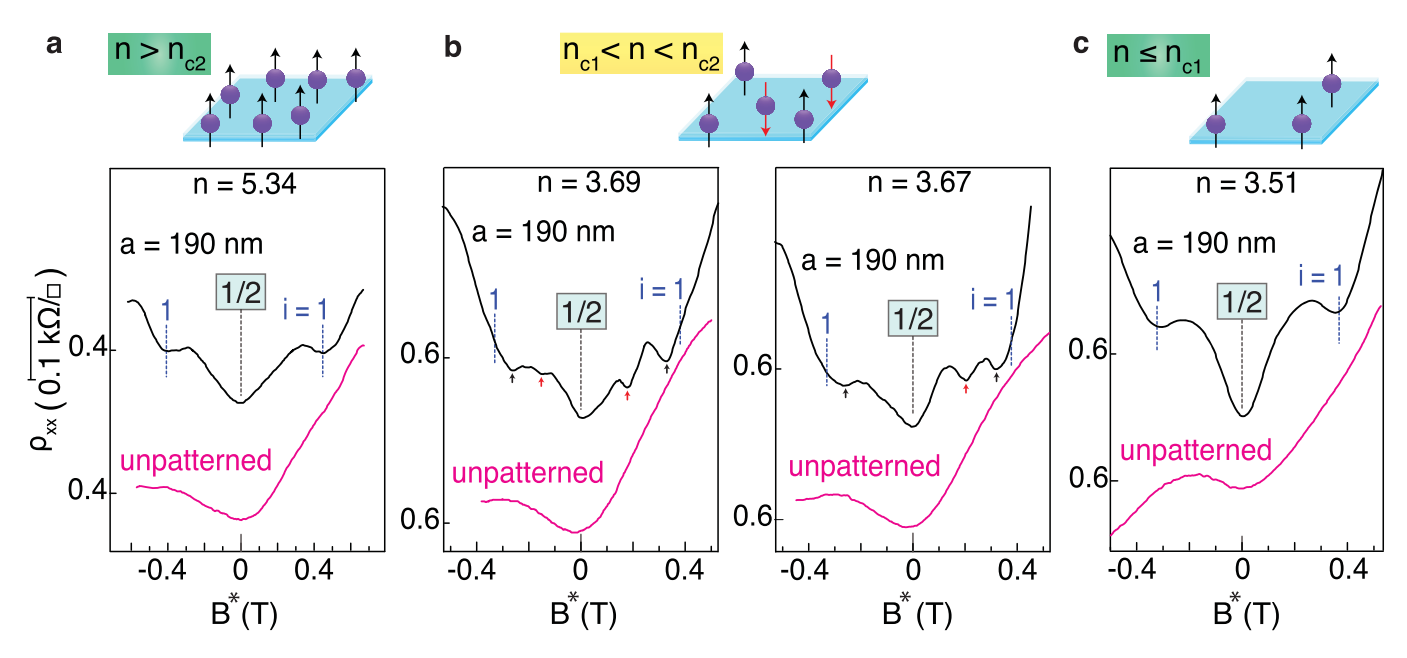
The authors declare no competing interests.

Additional information

Extended data is available for this paper at https://doi.org/10.1038/s41567-020-1000-z. **Supplementary information** is available for this paper at https://doi.org/10.1038/s41567-020-1000-z.

Correspondence and requests for materials should be addressed to M.S.H., J.K.J. or M.S. Reprints and permissions information is available at www.nature.com/reprints.

LETTERS NATURE PHYSICS



Extended Data Fig. 1 | Comparison between the patterned and unpatterned sections of the Hall bar. Comparison between the patterned and unpatterned sections of the Hall bar. **a-c**, Magneto-resistance traces for four densities, taken in the patterned (a = 190 nm) and unpatterned sections, are shown. Traces are vertically offset for clarity. While we observe clear geometric resonance minima flanking v = 1/2 in the traces taken from the section patterned with an a = 190 superlattice, the unpatterned section traces do not exhibit any such features, as expected. The cartoons in the upper panels show the spin configurations for different densities.